A novel hydrogel scaffold for periodontal ligament stem cells

KRISZTINA NAGY[1], ORSOLYA LÁNG[2], JÚLIA LÁNG[2], KATALIN PERCZEL-KOVÁCH[1,3], SZABOLCS GYULAI-GAÁL[4], KRISTÓF KÁDÁR[1], LÁSZLÓ KŐHIDAI[2], GÁBOR VARGA[1,*]

[1]Department of Oral Biology, Semmelweis University, Budapest, Hungary
[2]Department of Genetics, Cell- and Immunobiology, Semmelweis University, Budapest, Hungary
[3]Department of Community Dentistry, Semmelweis University, Budapest, Hungary
[4]Department of Oral Diagnostics, Semmelweis University, Budapest, Hungary
*Corresponding author: Gábor Varga, PhD, DSc; Department of Oral Biology, Semmelweis University, Nagyvárad tér 4, H-1089 Budapest, Hungary; Phone: +36 1 210 4415; Fax: +36 1 210 4421; E-mail: varga.gabor@dent.semmelweis-univ.hu

(Received: December 21, 2017; Revised manuscript received: March 5, 2018; Accepted: April 4, 2018)

Abstract: Periodontal ligament stem cells (PDLSCs) possess extensive regeneration potential. However, their therapeutic application demands a scaffold with appropriate properties. HydroMatrix (HydM) is a novel injectable peptide nanofiber hydrogel developed recently for cell culture. Our aim was to test whether HydM would be a suitable scaffold for proliferation and osteogenic differentiation of PDLSCs. PDLSCs were seeded on non-coated or HydM-coated surfaces. Both real-time impedance analysis and cell viability assay documented cell growth on HydM. PDLSCs showed healthy, fibroblast-like morphology on the hydrogel. After a 3-week-long culture in osteogenic medium, mineralization was much more intense in HydM cultures compared to control. Alkaline phosphatase activity of the cells grown on the gels reached the non-coated control levels. Our data provided evidence that PDLSCs can adhere, survive, migrate, and proliferate on HydM and this gel also supports their osteogenic differentiation. We first applied impedimetry for dental stem cells cultured on a scaffold. HydM is ideal for *in vitro* studies of PDLSCs. It may also serve not only as a reference material but also in the future as a promising biocompatible scaffold for preclinical studies.

Keywords: stem cell, HydroMatrix, periodontal ligament, cell proliferation, impedimetry, osteogenic differentiation

Introduction

Dental stem cell (SC)-based therapies could provide new opportunities in the field of regenerative medicine. The fact that SCs exist in periodontal tissues became evident in 2004 when Seo et al. [1] first succeeded in isolating periodontal ligament stem cells (PDLSCs). This mesenchymal SC type possesses multipotent differentiation capacities including osteogenic [1], adipogenic [1], chondrogenic [2], and myogenic [3] ones. Beyond these mesenchymal lineages, PDLSCs can also be differentiated into neuronal phenotype [3] due to their ectomesenchymal origin. The wide spectrum of their regeneration potential makes these cells ideal candidates for regeneration therapy.

To be useful for tissue regeneration therapy, an ideal scaffold should fulfill the following three criteria: (1) biocompatibility, (2) biodegradability, and (3) three-dimensional structure similar to the natural environment of the cells, e.g., extracellular matrix (ECM) [4]. Intensive research to find structures for biomedical application found that hydrogels are the most promising scaffolds [4–6]. Hydrogels are cross-linked, three-dimensional hydrophilic polymer networks that are insoluble in water but can absorb large amounts of water or biological fluids [7]. Among hydrogels, increasing attention is paid to *in situ* gelling hydrogels. The great advantage of these gels is that they are injectable and spontaneous gel formation occurs under physiological conditions [8]. Due to the chemical similarity to ECM proteins, self-assembling peptide hydrogels are the most suitable for mimicking the natural ECM [9]. However, for clinical application of periodontal SCs, a scaffold with appropriate properties is also required. In the preclinical studies of dental SCs, investigations are

usually performed on uniquely manufactured scaffolds specific for every laboratory. Indeed, there is high need for scaffolds with standard composition and manufacturing, which may serve as reference material for the reliable comparison of different scaffolds. At present, no scaffold materials are commercially available for tissue regeneration applications of PDLSCs [10].

HydroMatrix (HydM; Sigma-Aldrich, St. Louis, MO, USA) is a synthetic peptide nanofiber scaffold that self-assembles from soluble precursors into a three-dimensional hydrogel in response to increased temperature or ionic strength. This scaffold was developed for cell culture and tissue engineering purposes and has been shown to support the proliferation of many cell types, including neural SCs, fibroblasts, and keratinocytes [11]. Their rapid sol-gel transformation occurs at normal physiological temperature upon addition of standard cell culture medium. However, as a cell culture scaffold, HydM has been used so far only once in a study investigating ECM synthesis of human primary chondrocytes [12]. The aim of this study was to test whether HydM would be a suitable scaffold for the proliferation and differentiation of PDLSCs, to characterize the interactions between the scaffold and periodontal SCs, and to study the dynamics of cell adhesion, proliferation, and differentiation on HydM. Real-time and high frequency sampling (up to 1 measurement/s) of cell adhesion allowed us to follow even minor cell physiological responses in the populations of PDLSCs. Among the multipotent differentiation capacity of these dental SCs, we addressed the osteogenic direction for its potential future usefulness in the dental field, as loss of alveolar bone tissue contributes to the development of periodontitis.

Materials and Methods

Hydrogel scaffold preparation

HydroMatrix™ (Sigma-Aldrich) was purchased as a lyophilized powder. About 1% (w/v) stock solution was prepared according to the manufacturer's instructions, except that pH was adjusted to 7 with NaOH prior to the cell culture experiments, as the pH of the aqueous solution of HydM is around 2.5. Of the 0.5% working solution, 25 µl was used per well in 96-well plates and 50 µl in eight chamber slides. Gel formation was initiated by adding 1–2 volumes of expanding medium, resulting in 0.25% or 0.17% gel concentrations, respectively. After incubation for 1 h at 37 °C, the medium was carefully changed twice during the next 2 h before adding the cells.

Cell isolation and culture

Impacted third molars were surgically removed from healthy young adults at the Department of Dentoalveolar Surgery, Semmelweis University, under approved ethical guidelines set by the Ethical Committee of the Hungarian Medical Research Council. PDLSCs were isolated as previously described [13] with the following minor modifications. The tissue samples were digested in collagenase type I solution (1 mg/ml; Sigma-Aldrich) as well as the expanding medium contained 10% fetal bovine serum (Gibco, Grand Island, NY, USA) and was not supplemented with L-ascorbic acid 2-phosphate.

The authors of this manuscript have certified that they comply with the principles of ethical publishing in Interventional Medicine & Applied Science: Szél Á, Merkely B, Hüttl K, Gál J, Nemes B, Komócsi A: Statement on ethical publishing and scientific authorship. IMAS 2, 101–102 (2010).

Measurement of adhesion and proliferation using real-time impedance analysis

Adhesion and proliferation of the SCs were characterized using an xCELLigence SP system (Roche, Indianapolis, IN, USA), based on the real-time monitoring of electrical impedance on a microelectrode integrated 96-well cell culture plate (E-plate) (Roche). First, the surface of the gold electrodes was treated by 0.17% or 0.25% HydM gel. Formation of the hydrogel and manipulations including medium exchange steps were continuously monitored. Non-coated wells were used as reference and to detect the native adhesion profile of the cells. PDLSCs were seeded in E-plates at 5×10^4, 10^5, and 2.5×10^5 cells/ml densities in 100 µl of expanding medium per well. Cell adhesion and proliferation were followed for 24–72 h by impedimetry, a method that describes the surface area covered by the cells. The detected impedance depends on the number and spreading of cells adhered to the surface of the electrodes. This value is calculated as a relative and dimensionless value, using the following formula:

$$\mathrm{CI} = \frac{(Z_i - Z_0)}{F_i},$$

where CI represents "cell index," Z_i is the impedance at an individual point of time during the experiment, Z_0 is the impedance at the start of the experiment, whereas F_i is a constant coefficient to the system depending on the frequency of AC ($F_{10\mathrm{kHz}} = 15$). Therefore, CI is calculated from the change in impedance reflected to the baseline.

Beyond CI, delta cell index (ΔCI) was also used to characterize intensity of cell adhesion/proliferation. ΔCI is calculated as the CI at a given time point plus a delta value:

$$\Delta\mathrm{CI} = \mathrm{CI} + (\Delta\mathrm{CI}_{\mathrm{reference}} - \mathrm{CI}_{\mathrm{delta\_time}}).$$

In data analysis, the integrated software RTCA 1.2 (Roche) of xCELLigence SP was applied in calculations

of CI and ΔCI values at the individual time points. Each value represents the mean of at least three parallel measurements.

Cell viability assay

The cell proliferation reagent WST-1 [2-(4-iodophenyl)-3-(4-nitrophenyl)-5-(2,4-disulfophenyl)-2H-tetrazolium] (Roche) was used to measure cell viability. This colorimetric assay is based on the measurement of the mitochondrial dehydrogenase enzyme activity similar to conventional [3-(4,5-dimethylthiazol-2-yl)-2,5-diphenyltetrazolium bromide] (MTT) or [2,3-bis-(2-methoxy-4-nitro-5-sulfophenyl)-2H-tetrazolium-5-carboxanilide] (XTT) assays, but the water soluble tetrasolium salt [3-(4,5-dimethylthiazol-2-yl)-2,5-diphenyltetrazolium bromide] (WST-1) reagent has several advantages. In contrast to MTT, WST-1 yields water-soluble cleavage product. Compared to XTT, WST-1 shows higher sensitivity and broader linear range in readouts. About 10^4 PDLSCs in 100 µl medium were seeded into each well of 96-well plates coated or not with HydM. After 24, 48, and 72 h, WST-1 reagent was diluted at a 1:20 ratio with αMEM medium (containing no phenol red) and incubated with the cells for 2 h at 37 °C. Absorbance of the supernatants was then measured at 450 nm with a reference wavelength of 655 nm, using the Bio-Rad Model 3550 microplate reader (Hercules, CA, USA). Background control values were measured on supernatants of gels without seeded cells. Each value reported represents the mean of at least three parallel measurements.

Cell morphology studies

Cellular morphology on the surface of HydM was investigated under an inverted phase contrast microscope (Nikon TMS, Tokyo, Japan). Photomicrographs were taken by a high performance CCD camera (COHU, San Diego, CA, USA) using the Scion Image software (Scion Corporation, Frederick, MD, USA).

Osteogenic differentiation

Osteogenic differentiation was induced as previously described [13]. PDLSCs were seeded in 96-well plates (10^4 cells/well) or in eight-chamber slides (2×10^4 cells/chamber), which were either coated or uncoated with 0.25% HydM gel. Osteogenic medium was replaced twice a week (without passaging) for 3 weeks.

Alkaline phosphatase (ALP) activity was measured 1–3 weeks after osteogenic induction according to a previously reported protocol [14], with slight modifications. First, the cells growing in 96-well plates were lysed in 100 µl/well of 1.5 M 2-amino-2-methyl-1-propanol (pH ~ 10.5; Sigma-Aldrich) for 10 min. Then, 100 µl of ALP yellow liquid substrate (Sigma-Aldrich) was added to each well. After incubation at 37 °C for 20 min, the absorbance of the yellow end product yielded by the p-nitrophenylphosphate (pNPP) → p-nitrophenol (pNP) reaction was measured by a microplate reader (Bio-Rad Model 3550) at 405 nm. Unknown samples were quantified against a calibration curve consisting of serial dilutions of pNP (Sigma-Aldrich).

Mineralization nodules resulting from osteogenic differentiation were detected at the end of the third week by von Kossa staining through staining with a 5% $AgNO_3$ solution for 30 min.

Real-time RT-PCR

For quantitative RT-PCR, PDLSCs were seeded in 24-well plates (4×10^4 cells/well), which were coated or uncoated with 0.25% HydM gel. Osteogenic differentiation was induced 1 day after cell seeding as described above. On days 0, 3, and 7, total RNA was isolated from four parallel wells of each biological sample using the Nucelospin RNA II kit (Macherey-Nagel, Düren, Germany). RNA concentration was determined by a NanoDrop ND-1000 spectrophotometer (NanoDrop Technologies, Wilmington, DE, USA). RNA integrity was verified by gel electrophoresis.

cDNA was synthesized using the Maxima First Strand cDNA Synthesis Kit (Thermo Scientific, Waltham, MA, USA) from 1 µg total RNA per sample in a total volume of 20 µl. TaqMan® Gene Expression Assays specific for the early osteogenic marker genes ALP (Hs01029141_g1), Runt-related transcription factor 2 (Runx2; Hs00231692_m1), and osterix (SP7; Hs01866874_s1), and for the endogenous control glyceraldehyde 3-phosphate dehydrogenase (GAPDH; Hs99999905_m1) were selected from the Applied Biosystems Assay on Demand database. PCR amplifications were carried out using Taqman Universal Mastermix II (Applied Biosystems, Budapest, Hungary) in a final volume of 20 µl. For the real-time detection of fluorescence signals from the 5′-fluorescein-labeled minor groove binder probe during the PCR amplification, a StepOne® Real-Time PCR System (Applied Biosystems) was used with the default settings (50 °C for 2 min and 95 °C for 10 min, followed by 40 cycles of 95 °C for 15 s and 60 °C for 1 min). Changes in gene expression were determined using the relative expression values normalized to the level of GAPDH from the same sample. For each experimental condition, relative expression values were calculated from six parallel measurements.

Statistical analyses

Data are expressed as mean ± standard errors of the mean from at least three independent experiments.

Statistical evaluation of the data was carried out by the STATISTICA software applying Kruskal–Wallis non-parametric analysis of variance followed by median test. A difference was considered to be statistically significant, if $p < 0.05$.

Results

Cell adhesion and proliferation on uncoated plastic surface

Electrical impedance (Z) measured in living cells is due to the insulator property of the intact surface membrane. Cell adhesion and proliferation can be characterized by impedimetry. This method is based on the fact that the measured CI is influenced mainly by three parameters: (1) number, (2) viability, and (3) morphology (spreading area) of the adhered cells. To the best of our knowledge, this is the first study when impedimetry is used to study the adhesion and proliferation of dental SCs. We first characterized the cell adhesion and proliferation profile of PDLSCs *(Fig. 1A)* on uncoated plastic surface. We found that the kinetics of the change in ΔCI was dependent on the initial cell-seeding density. In each applied seeding density, a local maximum was observed 2 h after cell seeding. After this local maximum, the kinetics of the change in ΔCI was found to be dependent on the initial cell-seeding density. At 5,000 cells/well, the ΔCI of PDLSCs slowly but gradually increased until the end of the observed period. On the contrary, higher seeding densities resulted in no substantial change ΔCI during the second and third days of incubation *(Fig. 1A)*. To validate our impedimetry measurements, cell survival was also tested by viability assay *(Fig. 1B)*. Similar to ΔCI data, cell viability showed no significant changes during the 3-day-long experiments after seeding cells with a density of 10,000 cells/well.

Cell adhesion and proliferation on HydM-coated surface

Attachment and then the growth of PDLSCs was also detected by impedimetry on HydM-coated surfaces as well *(Fig. 1C)*. On surfaces coated with HydM, changes in impedance after seeding were much slower due to the increased ohmic resistance of the gel. The initial increase in CI shows that PDLSCs could migrate through the gel consisting of HydM and successfully reach the surface of the gold electrodes located at the bottom of the wells of the 96-well culture plates. At the higher applied gel concentration (2.5 mg/ml), higher ΔCI values were measured than in the less concentrated gel, and this difference increased over time. The continuously increasing ΔCI values after 24 h indicate that PDLSCs were able to proliferate and further adhere to the surface

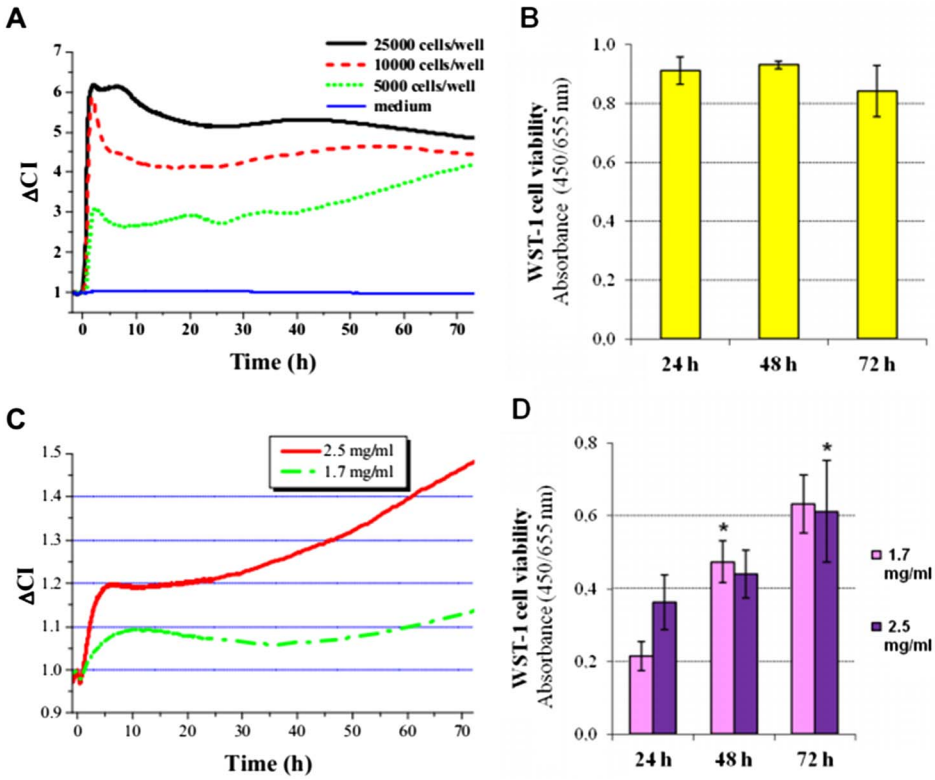

Fig. 1. Cell adhesion and proliferation of PDLSCs on non-coated (A, B) and HydroMatrix-coated (C, D) surfaces. Real-time impedance analysis (A, C) were carried out using an xCELLigence system. Cell viability was assessed by WST-1 assay (B, D) at a seeding density of 10,000 cells/well. Values are given as mean ± standard errors of the mean (SEM). *$p < 0.05$ compared to data gained 24 h after cell seeding

on the more concentrated HydM indicating that it provided better conditions for the PDLSCs than the softer gel. Using the WST-1 cell viability assay, we could demonstrate proliferation of PDLSCs on both HydMs *(Fig. 1D)*. PDLSCs on day 1 showed substantially higher viability on the 2.5 mg/ml gel compared to the 1.7 mg/ml gel, whereas later time points indicated that PDLSCs could proliferate in both gels. It is important to note that the measurement of CI by the xCELLigence system detects not only adhesion of the individual cells but the CI is also proportional with the number of living cells around the electrode. Thereby, it monitors a more complex biological response than the viability assay alone, which is based on the detection of mitochondrial constitutive enzyme activity. Moreover, in the initial stages, CI primarily reflects adhesion, while later on, it is determined by the invasive capacity of the cells as well.

Cellular morphology on non-coated and HydM-coated surfaces

Cellular morphology and surface covering of the different coatings were also followed by taking serial photographs under a phase contrast microscope *(Fig. 2)*. Increasing cell numbers over time can be observed on the micrographs independently of the presence of surface coating, although cell numbers on day 1 were visibly higher on the non-coated surface *(Fig. 2)*. PDLSCs displayed the same fibroblast-like morphology on HydM-coated surfaces, which is typical for these cells when cultured on normal plastic culture dishes. On non-coated surfaces, PDLSCs formed a confluent layer already on the first day and grew into multiple layer arrangement by day 3. The scaffold consisting of HydM also enabled three-dimensional structure formation of the cells. Our morphological observations are in good accordance with the above described results of the viability assay *(Fig. 1B and D)*, since both methods showed well cells adhered to the HydM gels.

Osteogenic differentiation on HydM-coated surfaces

As described above, cells grown on gels with 2.5 mg/ml HydM concentration displayed higher ΔCI values with more cells on the gel surface. Thus, this gel concentration was selected for the differentiation experiments. As an indicator of osteogenic differentiation, ALP activity was measured weekly during the 3-week-long culture in osteogenic medium. ALP activity was undetectable on day 0 in both control and HydM groups. ALP activity of PDLSCs on days 7 and 14 was significantly lower on HydM than on

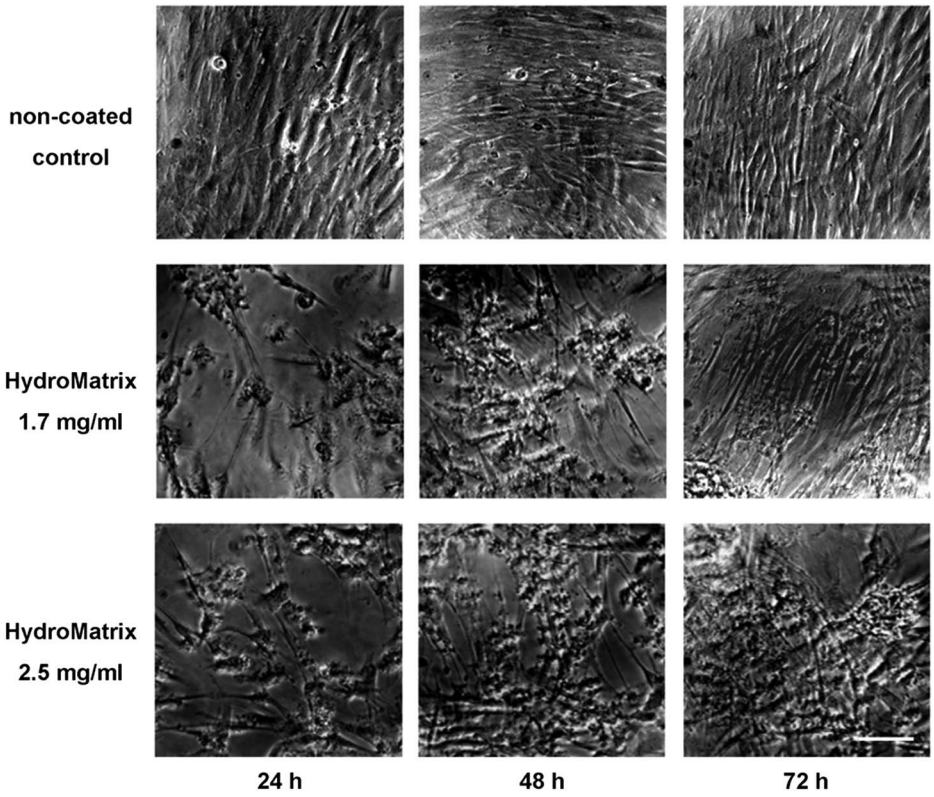

Fig. 2. Morphology of PDLSCs on non-coated and HydroMatrix (HydM)-coated surfaces studied by phase contrast microscopy. Healthy, fibroblast-like cellular morphology can be observed both on plastic and gel surfaces. Although the cell density is lower on HydM-coated surfaces than on non-coated surface after 24 h, remarkable cell proliferation occurs during the next 2 days on the gel surfaces. After 72 h, PDLSCs on HydM reach high cell density and form multilayer arrangements similar to cells growing on plastic surface. The seeding density was 10,000 cells/well. Bars indicate 100 μm

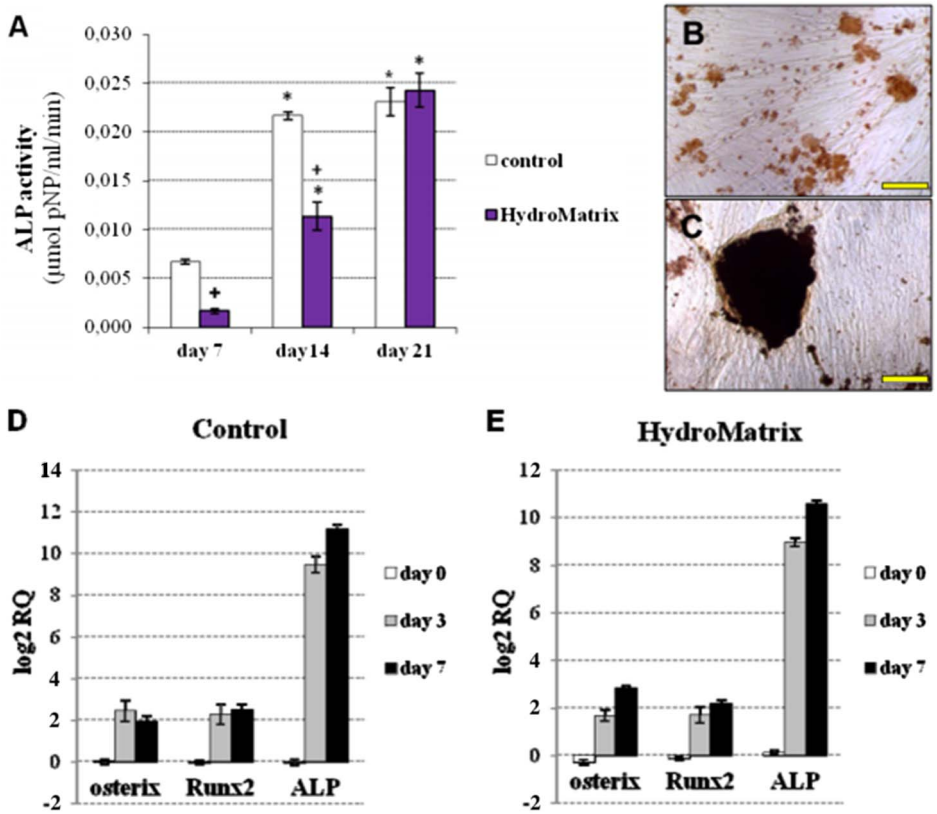

Fig. 3. Osteogenic differentiation of PDLSCs on non-coated and HydroMatrix (HydM)-coated surfaces. Alkaline phospatase (ALP) activity (A) was measured by pNPP cleavage test. $^{*}p < 0.05$ compared to day 7. $^{+}p < 0.05$ compared to control. von Kossa staining of PDLSC cultures on non-coated (B) and HydM-coated (C) surfaces on day 21 of differentiation. Bars indicate 100 μm. mRNA expression pattern of early markers in PDLSCs grown on tissue culture plastic (D) and HydM-coated (E) surfaces during osteogenic differentiation. Real-time RT-PCR was carried out using total RNA samples harvested on days 0, 3, and 7 of osteogenic differentiation on non-coated and HydM-coated surfaces. Expression of ALP, Runt-related transcription factor 2 (Runx2), and osterix (SP7) genes was normalized to the glyceraldehyde 3-phosphate dehydrogenase (GAPDH) housekeeping gene expression levels and expressed as fold change relative to the day 0 value of the non-coated control. Data are presented as means of six parallel experiments and error bars indicate standard errors of the mean (SEM)

non-coated surfaces, but it reached the control level by day 21 *(Fig. 3A)*. Thus, during the first 2 weeks of osteogenic differentiation, the increase of ALP activity was delayed by HydM; but at the end of the third week, ALP activities on HydM and plastic became similar. On plastic surfaces, mineral deposits were small with a lower calcium content *(Fig. 3B)*, while large mineralized nodules were detected by von Kossa staining on HydM-coated surfaces *(Fig. 3C)*.

To monitor the changes in mRNA levels of the early osteogenic marker genes ALP, Runx2, and osterix, we performed real-time PCR assays at three different time points during the first week of differentiation *(Fig. 3D and E)*. The expression of each target gene was normalized to that of the GAPDH housekeeping gene, and expressed as fold change relative to day 0 values of the non-coated control sample. The expression of ALP elevated sharply by day 7, reaching 2,300- and 1,600-fold increase compared to day 0 control values in PDLSCs cultured on non-coated and HydM-coated surfaces, respectively. The changes in Runx2 expression were also significant by day 7 compared to day 0 control in cultures on plastic and hydrogel-coated surfaces, reaching 5.6- and 4.5-fold elevations, respectively. The relative expression of osterix increased by approximately 3–7 fold over starting values on plastic and on hydrogel-coated surfaces at both time points in PDLSCs, respectively.

As expected, considerable morphological changes were observed by phase contrast microscopy during osteogenic differentiation *(Fig. 4)*. On non-coated surfaces, PDLSCs formed confluent monolayers after 1 week, followed by the formation of multilayer structures. By day 14, PDLSCs formed mineral deposits, easily detected as small dark spots even without staining. On HydM, PDLSCs formed rounded cell clusters by day 7 of the differentiation protocol. These clusters attained large size during the next 2 weeks and had an increasing number of dark deposits.

Discussion

The aim of this study was to test whether HydM could serve as a suitable scaffold for PDLSC proliferation and

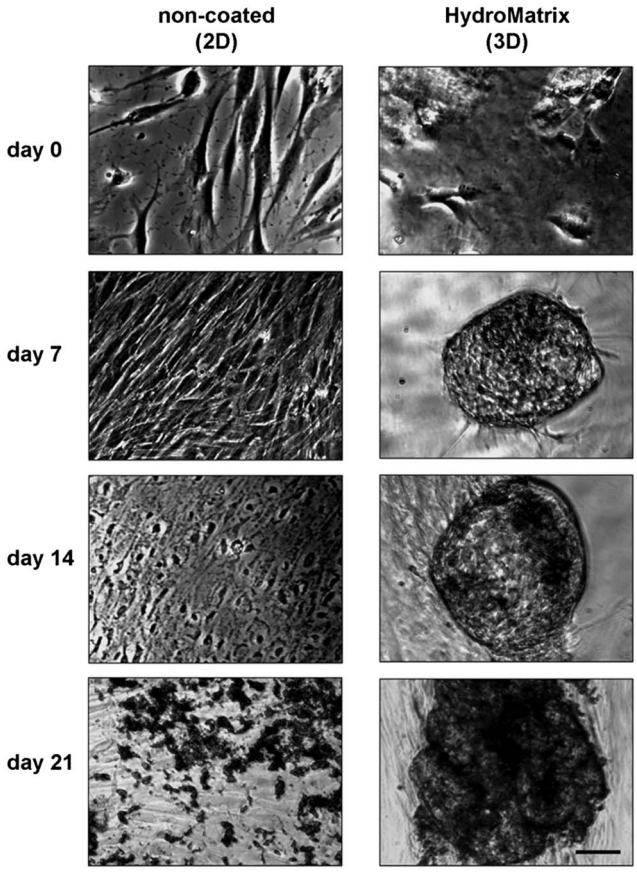

Fig. 4. Morphological changes during osteogenic differentiation of PDLSCs on non-coated and HydroMatrix (HydM)-coated surfaces. Before osteogenic induction (day 0), low cell density and normal, fibroblast-like morphology can be observed both on plastic and gel surfaces. During the 3 weeks of the osteogenic differentiation, cell density increases. On plastic surface, the cells form multiple layers and significant amount of mineral deposits (dark spots) by day 21. In HydM, spherical cell clusters can be found from day 7 containing more and more mineralized matrix from day 14. Bars indicate 100 μm

osteogenic differentiation *in vitro*. Real-time impedimetry was used to measure CI, a complex value for cell adhesion and proliferation of PDLSCs. We applied this non-invasive cell physiology technique to allow real-time high frequency (up to 1/s) measurement of impedance, which enables the detection of even minor physiological responses of cell populations [15, 16]. To our knowledge, this study is the first report on cell-scaffold interactions and on dynamics of cell adhesion and proliferation obtained by real-time impedimetry on dental originated mesenchymal SCs.

Our finding that the adhesion of human PDLSCs on tissue culture plastic is accompanied by an increase of the CI to a temporary maximum 2–3 h after plating is in accordance with previous studies on human gingival fibroblasts [17, 18]. The same proliferation profile was also detected in mesenchymal SCs derived from bone marrow [19], chorion [20], and pancreas [21]. This phenomenon can be explained by a well-known property of fibroblast-like cells that individual cells initially spread out and display a typical morphology with processes only a few hours later. These stages of adhesion were consistently observed by various investigators for gingival fibroblasts [22], periodontal ligament fibroblasts [23], and bone marrow mesenchymal SCs [24]. The increasing impedance in PDLSC cultures after 8–10 h reported in our present experiment suggests that these cells complete the adhesion phase in 10 h and the proliferation phase begins afterward. Similar to our results, a local minimum in CI was measured in human ginigival fibroblasts at 7–10 h [17]. We validated our real-time impedance analysis with a conventional end-point assay, such as the WST-1 viability assay, which is based on the measurement of mitochondrial dehydrogenase enzyme activity. In accordance with this, a recent study also revealed a close match between xCELLigence data and results of the viability assay using another reagent [17].

Both impedimetry and cell viability assay underlined that PDLSCs are capable to adhere and proliferate on HydM as well. Cell adhesion and migration of another dental SC type, the SCs from human exfoliated deciduous teeth (SHED) was also recently demonstrated in a biodegradable peptide hydrogel [25]. Our finding that gel concentration does not dramatically influence cell viability is in accordance with results on the growth of dental pulp stem cell cultures (DPSCs) in Puramatrix^{TM} (PuraM, BD, Franklin Lakes, NJ, USA) [26]. We have to note although, that the higher applied concentration of HydM supported cell adhesion and spreading more than the lower applied one. Therefore, fine tuning of the physical and chemical characteristics of the applied gel seems to be very important to elaborate optimal conditions for cell-scaffold interactions. The healthy morphology of PDLSCs observed on HydM-coated surfaces indicates that HydM provides an ideal environment for the survival and well-being of these SCs. Structurally, PDLSC clusters in HydM are similar to those found in case of DPSCs in PuraM [26], suggesting that both HydM and PuraM are suitable as potentially biocompatible scaffolds for SC cultures of dental origin.

Among the multipotent differentiation capacity of PDLSCs, we addressed the osteogenic direction as it could be useful in the future for alveolar bone regeneration during periodontitis. Osteogenic differentiation of the cells was verified by measurement of ALP activity and von Kossa staining. Even though, during the first 2 weeks of differentiation, ALP activity was significantly lower on HydM compared to non-coated surface, it reached control levels by day 21. The observed increase in ALP activity during 3 weeks of osteogenic differentiation is in accordance with previous studies on DPSCs and SHEDs cultured on another type of peptide hydrogel [14].

Osteogenic differentiation of PDLSCs on both non-coated and HydM-coated surfaces was confirmed by real-time PCR studies. The changes in the expression of genes regulating early events during osteoblast differentiation, such as ALP, Runx2, and osterix [27, 28], were studied 0, 3, and 7 days after the osteogenic induction. In the literature, only very few data are available on the changes in the expression of these genes during the first 7 days during *in vitro* osteogenesis. We demonstrated a sharp increase in ALP expression during the first 7 days of osteogenic differentiation on both HydM and plastic surfaces, which is in agreement with recently published results on PDLSCs after 1 week of differentiation [29]. Similar to our observations, another study by Wang et al. [30] revealed significant upregulation of osterix and Runx2 in SCs isolated from the apical papilla, 3 days after the osteogenic induction. Our finding that Runx2 expression significantly elevated during osteogenic differentiation is in accordance with previous publications by Lindroos et al. [31], although they performed qPCR measurements only after 2 weeks of differentiation. The relatively lower expression level of osterix compared to Runx2 that we found in PDLSCs can be explained by the downstream action of osterix compared to Runx2 in the osteoblast differentiation process [32].

Additional to the above discussed results, using phase contrast microscopy, we compared two-dimensional growth on non-coated surfaces with three-dimensional growth observed on HydM. We found that PDLSC formed clusters during osteogenic differentiation that later became von Kossa-positive spheric mineralizing structures. To the best of our knowledge, this is the first report to describe such morphological changes of dental originated mesenchymal SCs during *in vitro* mineralization.

Conclusions

This is the first study of dental SCs cultured on HydM gel and simultaneously this is the first report on impedimetric analysis of these cells growing on a scaffold material. The present data provide evidence that PDLSCs can adhere, migrate, survive, proliferate, and differentiate into osteogenic direction on the HydM gel. Consequently, HydM may serve as a standard reference material for dental SC-scaffold interaction studies. It may also serve as a scaffold for the use of periodontal SCs in regenerative dental and orthopedic medicine. Future *in vivo* preclinical studies using the HydM gel would be the next step toward this aim.

* * *

Funding sources: This work was supported by the Hungarian National Scientific Research Fund (OTKA-NKTH CK-80928) and Hungarian Human Resources Development Operational Programme (EFOP-3.6.2-16-2017-00006).

Authors' contribution: GV contributed to research conception, coordination of the project, and critical revision of the manuscript. KN contributed to cell culture, differentiation, viability, morphology, and PCR studies, data collection and processing, and preparation of the manuscript. KP-K contributed to cell isolation, culture, differentiation, and viability studies. KK contributed to experimental design, data handling, and statistical analysis. LK contributed to coordination of impedimetric experiments and preparation of the manuscript. OL contributed to impedimetric investigations, data collection, and processing. JL contributed to the impedimetric investigations. SG-G contributed to surgical removal of wisdom teeth. All authors read and approved the final version of the manuscript.

Conflict of interest: The authors declare no conflict of interest.

Acknowledgements: The authors would like to thank Ms. Karola Kálló and Dr. Anna Földes for their help in cell isolation and design of PCR experiments. They would also like to thank Dr. Lívia Fülöp (Department of Medical Chemistry, University of Szeged) for the valuable discussions regarding gel preparation. This article is dedicated to the memory of Karola Kálló.

References

1. Seo BM, Miura M, Gronthos S, Bartold PM, Batouli S, Brahim J, Young M, Robey PG, Wang CY, Shi S: Investigation of multipotent postnatal stem cells from human periodontal ligament. Lancet 364, 149–155 (2004)
2. Gay IC, Chen S, Macdougall M: Isolation and characterization of multipotent human periodontal ligament stem cells. Orthod Craniofac Res 10, 149–160 (2007)
3. Huang CY, Pelaez D, Dominguez-Bendala J, Garcia-Godoy F, Cheung HS: Plasticity of stem cells derived from adult periodontal ligament. Regen Med 4, 809–821 (2009)
4. Drury JL, Mooney DJ: Hydrogels for tissue engineering: Scaffold design variables and applications. Biomaterials 24, 4337–4351 (2003)
5. Baroli B: Hydrogels for tissue engineering and delivery of tissue-inducing substances. J Pharm Sci 96, 2197–2223 (2007)
6. Hoffman AS: Hydrogels for biomedical applications. Adv Drug Deliv Rev 54, 3–12 (2002)
7. Peppas NA, Bures P, Leobandung W, Ichikawa H: Hydrogels in pharmaceutical formulations. Eur J Pharm Biopharm 50, 27–46 (2000)
8. Van Tomme SR, Storm G, Hennink WE: In situ gelling hydrogels for pharmaceutical and biomedical applications. Int J Pharm 355, 1–18 (2008)
9. Webber MJ, Kessler JA, Stupp SI: Emerging peptide nanomedicine to regenerate tissues and organs. J Intern Med 267, 71–88 (2010)
10. Rodriguez-Lozano FJ, Insausti CL, Iniesta F, Blanquer M, Ramirez MD, Meseguer L, Meseguer-Henarejos AB, Marin N, Martinez S, Moraleda JM: Mesenchymal dental stem cells in regenerative dentistry. Med Oral Patol Oral Cir Bucal 17, e1062-7 (2012)
11. HydroMatrix Peptide Hydrogel. (2012) [cited 11.06.2014]. Retrieved from http://www.sigmaaldrich.com/life-science/stem-cell-biology/3d-stem-cell-culture/hydromatrix-peptide.html
12. Stoppoloni D, Politi L, Dalla Vedova P, Messano M, Koverech A, Scandurra R, Scotto D'abusco A: L-carnitine enhances extracellular matrix synthesis in human primary chondrocytes. Rheumatol Int 33, 2399–2403 (2013)
13. Kadar K, Kiraly M, Porcsalmy B, Molnar B, Racz GZ, Blazsek J, Kallo K, Szabo EL, Gera I, Gerber G, Varga G: Differentiation potential of stem cells from human dental origin – Promise for tissue engineering. J Physiol Pharmacol 60, 167–175 (2009)

14. Galler KM, Cavender A, Yuwono V, Dong H, Shi ST, Schmalz G, Hartgerink JD, D'souza RN: Self-assembling peptide amphiphile nanofibers as a scaffold for dental stem cells. Tissue Eng Part A 14, 2051–2058 (2008)
15. Lajko E, Szabo I, Andody K, Pungor A, Mezo G, Kohidai L: Investigation on chemotactic drug targeting (chemotaxis and adhesion) inducer effect of GnRH-III derivatives in tetrahymena and human leukemia cell line. J Pept Sci 19, 46–58 (2013)
16. Leurs U, Lajko E, Mezo G, Orban E, Ohlschlager P, Marquardt A, Kohidai L, Manea M: GnRH-III based multifunctional drug delivery systems containing daunorubicin and methotrexate. Eur J Med Chem 52, 173–183 (2012)
17. Urcan E, Haertel U, Styllou M, Hickel R, Scherthan H, Reichl FX: Real-time xCELLigence impedance analysis of the cytotoxicity of dental composite components on human gingival fibroblasts. Dent Mater 26, 51–58 (2010)
18. Yalcin M, Barutcigil C, Umar I, Bozkurt BS, Hakki SS: Cytotoxicity of hemostatic agents on the human gingival fibroblast. Eur Rev Med Pharmacol Sci 17, 984–988 (2013)
19. Adamowicz J, Kloskowski T, Tworkiewicz J, Pokrywczynska M, Drewa T: Urine is a highly cytotoxic agent: Does it influence stem cell therapies in urology? Transplant Proc 44, 1439–1441 (2012)
20. Kim JH, Jekarl DW, Kim M, Oh EJ, Kim Y, Park IY, Shin JC: Effects of ECM protein mimetics on adhesion and proliferation of chorion derived mesenchymal stem cells. Int J Med Sci 11, 298–308 (2014)
21. Roshan Moniri M, Young A, Reinheimer K, Rayat J, Dai LJ, Warnock GL: Dynamic assessment of cell viability, proliferation and migration using real time cell analyzer system (RTCA). Cytotechnology 67, 379–386 (2014)
22. Pelegrini CB, Maia LP, De Souza SL, Taba M Jr, Palioto DB: Morphological, functional and biochemical characterization of canine gingival fibroblasts. Braz Dent J 24, 128–135 (2013)
23. Hamilton DW, Oates CJ, Hasanzadeh A, Mittler S: Migration of periodontal ligament fibroblasts on nanometric topographical patterns: influence of filopodia and focal adhesions on contact guidance. PLoS One 5, e15129 (2010)
24. Lavenus S, Berreur M, Trichet V, Pilet P, Louarn G, Layrolle P: Adhesion and osteogenic differentiation of human mesenchymal stem cells on titanium nanopores. Eur Cell Mater 22, 84–96; discussion 96 (2011)
25. Galler KM, Aulisa L, Regan KR, D'souza RN, Hartgerink JD: Self-assembling multidomain peptide hydrogels: Designed susceptibility to enzymatic cleavage allows enhanced cell migration and spreading. J Am Chem Soc 132, 3217–3223 (2010)
26. Cavalcanti BN, Zeitlin BD, Nor JE: A hydrogel scaffold that maintains viability and supports differentiation of dental pulp stem cells. Dent Mater 29, 97–102 (2013)
27. Komori T: Regulation of osteoblast differentiation by transcription factors. J Cell Biochem 99, 1233–1239 (2006)
28. Pan K, Sun Q, Zhang J, Ge S, Li S, Zhao Y, Yang P: Multilineage differentiation of dental follicle cells and the roles of Runx2 over-expression in enhancing osteoblast/cementoblast-related gene expression in dental follicle cells. Cell Prolif 43, 219–228 (2010)
29. Choi MH, Noh WC, Park JW, Lee JM, Suh JY: Gene expression pattern during osteogenic differentiation of human periodontal ligament cells in vitro. J Periodontal Implant Sci 41, 167–175 (2011)
30. Wang L, Yan M, Wang Y, Lei G, Yu Y, Zhao C, Tang Z, Zhang G, Tang C, Yu J, Liao H: Proliferation and osteo/odontoblastic differentiation of stem cells from dental apical papilla in mineralization-inducing medium containing additional KH(2)PO(4). Cell Prolif 46, 214–222 (2013)
31. Lindroos B, Maenpaa K, Ylikomi T, Oja H, Suuronen R, Miettinen S: Characterisation of human dental stem cells and buccal mucosa fibroblasts. Biochem Biophys Res Commun 368, 329–335 (2008)
32. Nakashima K, Zhou X, Kunkel G, Zhang Z, Deng JM, Behringer RR, De Crombrugghe B: The novel zinc finger-containing transcription factor osterix is required for osteoblast differentiation and bone formation. Cell 108, 17–29 (2002)